Available online at www.sciencedirect.com

SciVerse ScienceDirect

journal homepage: www.intl.elsevierhealth.com/journals/dema

Marginal analysis of resin composite restorative systems using optical coherence tomography

Gabriela Q.M. Monteiro[a,b,*], *Marcos A.J.R. Montes*[a], *Anderson S.L. Gomes*[b], *Claudia C.B.O. Mota*[c], *Sérgio L. Campello*[d], *Anderson Z. Freitas*[e]

[a] *Department of Restorative Dentistry, Universidade de Pernambuco – FOP/UPE, Camaragibe, PE, Brazil*
[b] *Department of Physics, Universidade Federal de Pernambuco – UFPE, Recife, PE, Brazil*
[c] *Graduate Program in Dentistry, Universidade Federal de Pernambuco – UFPE, Recife, PE, Brazil*
[d] *Graduate Program in Materials Science, Universidade Federal de Pernambuco – UFPE, Recife, PE, Brazil*
[e] *Center for Laser and Applications, Nuclear and Energy Research Institute – IPEN-CNEN/SP, São Paulo, SP, Brazil*

ARTICLE INFO

Article history:
Received 30 May 2010
Received in revised form
20 August 2011
Accepted 24 August 2011

Keywords:
Optical coherence tomography
Dental composite
Dental adhesive
Marginal integrity

ABSTRACT

Objectives. To analyze marginal integrity of resin composites dental restorations using optical coherence tomography (OCT).

Methods. Thirty extracted human premolars had occlusal cavities prepared and were randomly divided according to the restorative systems evaluated: Filtek P90™/P90 Adhesive System™, Filtek Z350™, and Filtek Z250™/Single Bond™ (3 M/ESPE). The teeth were then stored in the dark for 24 h in 0.9% saline solution. Restorations were finished and polished and stored again for 24 h before thermocycling (500 cycles, 5–55 °C). A commercially available OCT system was used (SR-OCT: OCP930SR/Thorlabs) with 930 nm central wavelength. Cross-sectional images were obtained every 250 μm and evaluated using Image J. A-scans were analyzed using the Origin 8.0 program, after a filter treatment using Matlab.

Results. The qualitative analysis of the internal margins did not observe gaps even after A-scan examination, although distinctive patterns were found for each restorative system. Penetration of Single Bond and Filtek P90 self-etch primer into dentin was also observed. A thick adhesive layer was found for Filtek P90 bonding agent.

Significance. Considering the characteristics of the OCT system, the setup used in this study was capable of evaluating the marginal integrity of resin composite restorations and detecting some interaction between dental bonding agents and dental substrates. OCT can be considered a promising method for the evaluation of the internal margins of restorations *in vivo*.

1. Introduction

Resin composites are now used as a restorative material because of their excellent mechanical and esthetic properties. However, one of the biggest problems associated with their use is inherent shrinkage during the polymerization reaction. The polymerization reaction of dimethacrylate monomers involves approximation for the formation of polymer molecules. Therefore, by the end of the polymerization

* *Corresponding author at*: R. Abel de Sá B. Cavalcanti, 161/502 – Casa Amarela, Recife, PE 52.061-300, Brazil. Tel.: +55 81 3075 4448/9996 6327; fax: +55 81 2126 8118.
E-mail address: gabrielaqueiroz@hotmail.com.br (G.Q.M. Monteiro).
0109-5641/$ – see front matter © 2011 Academy of Dental Materials. Published by Elsevier Ltd. All rights reserved.
doi:10.1016/j.dental.2011.08.400

process, the polymer molecule occupies a smaller space compared with that required by the monomer at the beginning of the reaction. This contraction can cause flaws in the integrity of the tooth–restoration interface, hence, microleakage, marginal discoloration, recurrent caries, postoperative sensitivity and enamel fractures can occur. All of these factors can reduce the longevity of the restoration.

Improvements have been developed over the years always with the goal of enhancing the properties and the longevity of the material in the oral cavity. Most of these changes have occurred in the filler particles; the chemistry behind the organic matrix has undergone little change since the pioneering work of Bowen in 1960. Virtually all commercially available resin composites use dimethacrylates such as TEGDMA, Bis-GMA or UDMA, all cured by an addition reaction of free radicals in their double bonds [1]. This is because the incorporation of a greater amount of inorganic filler particles promotes a reduction in the organic matrix concentration, responsible for polymerization shrinkage. One of the ways found to increase the concentration of these particles was through a reduction in size, which culminated in the development of nanoparticles for such applications [2,3].

The use of nanoscale particles did not necessarily lead to an increase in the concentration of inorganic fillers, but it did lead to improvements in polish retention. Thus, polymerization shrinkage using nanoparticles remains similar to that of their precursors, microhybrid resin composites [4].

In search of ways to further reduce polymerization shrinkage, innovations in resin monomers emerged as a new challenge. As a result, a new type of resin matrix was developed based on cyclic monomers. These hydrophobic monomers are composed of a siloxane backbone with oxirane rings, and for that reason are called siloranes [5]. According to the manufacturer, the main advantage of this new restorative system is its reduced polymerization shrinkage with mechanical properties similar to resins based on methacrylates. The lower shrinkage is a result of the fact that their reaction is based on the opening of their rings via a cationic reaction. This process allows a gain of space that overlaps the volume contraction that occurs in the subsequent step of the reaction, when the monomers form chemical bonds between them leading to polymer chain formation.

To be used as restorative materials, silorane-based resins need compatible bonding agents, which led to the development of an inherent two-step self-etch adhesive.

Evaluation of the marginal integrity of restorations can be accomplished using various methods. The most common method is the evaluation of marginal leakage by dye penetration, followed by observation of the margins under a stereoscopic microscope and/or scanning electron microscope (SEM). For SEM, sectioning of the tooth/restorations involved is required to assess the presence of internal cracks and irregularities, which does not allow evaluation of the marginal integrity *in vivo*. However, non-destructive analysis using SEM can be performed by obtaining epoxy replicas of the occlusal surface of the restoration [6].

In this context, optical coherence tomography (OCT) is a possible technique for analysis of the tooth–restoration interface. Introduced in medicine at the beginning of the 1990s, optical tomography has become a powerful method for image acquisition of internal structures of biological systems and materials. This method obtains sub-surface images in a non-invasive way using light rather than a magnetic field or x-radiation. OCT uses the optical properties (reflection and backscattering) for image generation. Its principle is similar to ultrasound, although the latter uses sound waves and the former uses light. Depending on the source spectral bandwidth, it is possible to obtain images with micrometer (μm) resolution. Furthermore, with the OCT system there is no need for direct contact between the probe or apparatus and the tissue under study or the immersion fluid, as light can easily pass through the air–tissue interface [7,8].

The optical setup consists of a Michelson interferometer with a low coherence broadband light source. The light generated in an OCT system is split into two arms: a sample arm, containing the item of interest, and a reference arm that contains a movable mirror.

The reflected light from the sample arm and from the reference arm are then recombined and focused by a spectrometer, where any degree of interference between the beams can be observed, but only if light from both arms have traveled the same optical distance [9,10].

Nowadays, superluminescent diodes (SLDs) are the preferred source for light generation in OCT systems. This light source produces a wide range of wavelengths, each one generating its own interference image. The intensity of the interference depends on scattering caused by changes in the structure of the tooth, for example. Areas of the sample that backscatter a lot of light will create greater interference than areas that do not. This reflectivity profile, called an A-scan, contains information about the spatial dimensions and location of structures within the item of interest. By making a series of A-scans, scanning transversely to the light beam, it is possible to obtain a two-dimensional map (B-scan) of the reflected light in each point of the scanned area. In other words, a cross-sectional tomographic image may be achieved by combining a series of A-scans along a line.

OCT has been used previously to evaluate gaps at the tooth–restoration interface. In that study, amalgam and composite restorations had intentional gaps (51–146 μm) made at the interface with an acetate tape. Optical microscope analysis confirmed the results revealed by OCT for the location and size of the gaps [11]. The aim of this laboratory study was to qualitatively evaluate the marginal integrity of the new silorane-based restorations under OCT, and to compare it with conventional methacrylate-based restorations. The hypotheses tested were: (1) OCT can be used as a diagnostic method for evaluating marginal integrity; (2) there are no differences in marginal integrity for the restorative systems tested.

2. Materials and methods

The materials, manufacturers, composition and batch numbers for the materials used in this study are listed in Table 1.

2.1. *Experimental setup*

A commercially available OCT system was used (Spectral Radar SR-OCT: OCP930SR/Thorlabs, New Jersey, USA). The

Table 1 – Composition, manufacturers and batch numbers of the materials studied.

Material	Composition: filler class, % weight, % volume	Manufacturer[a] (batch no.)	Restorative technique
Filtek Z250™	BisGMA, UDMA and BisEMA BisGMA, zirconia/silica: microhybrid, 82%, 60%	3M/ESPE (5WK)	2-mm increments; photoactivation for 20 s
Filtek Z350™	UDMA, TEGDMA and BisEMA, zirconia/silica and silica: nanoparticle, 78.5%, 59.5%	3M/ESPE (6EB)	2-mm increments; photoactivation for 20 s
Filtek P90™	Silorane resin, quartz filler and yttria fluoride, stabilizers, pigments: microhybrid, 76%, 55%	3M/ESPE (9CH)	2-mm increments; photoactivation for 40 s
Adper Single Bond 2™	BisGMA, HEMA, dimethacrylates, ethanol, water, photoinitiator system, methacrylate functional copolymer of polyacrylic and polyitaconic acids, 5-nm silica particles	3M/ESPE (9XE)	1. Etching with phosphoric acid 35%. Applied first to enamel and then to dentin. Wait 15 s and rinse for 30 s. Blot excess water using a humid cotton pellet 2. Immediately after blotting, apply a coat of adhesive with gentle agitation using fully saturated applicator for 20 s. Repeat the application. Gently air thin for 5 s to evaporate solvent. Photoactivation for 20 s
P90 System Adhesive™	*Self-etch primer*: Phosphorylated methacrylates, vitrebond copolymer, BisGMA, HEMA, water, ethanol, silane-treated silica filler, initiators, stabilizers	3M/ESPE (9BL)	1. Apply 1 coat of the self-etch primer using fully saturated applicator for 15 s with gentle agitation. Gently air thin to evaporate solvent and obtain an even film. Photoactivation for 10 s
	Bond: Hydrophobic methacrylates, phosphorylated methacrylates, TEGMA, silane-treated silica filler, initiators, stabilizers	3M/ESPE (9BH)	2. Apply the bond to the entire preparation using fully saturated applicator. Gently air thin until the bond is spread to an even film and does not move any longer. Photoactivation for 10 s

All composites were A2 color. BisGMA, bisphenol-glycidyl methacrylate; UDMA, urethanethyl dimethacrylate; TEGDMA, triethylene glycol dimethacrylate; BisEMA, bisphenol-polyethylene glycol dimethacrylate; HEMA, 2-hydroxyethylmethacrylate.
[a] 3M ESPE, St. Paul, MN, USA.

superluminescent diode (SLD) light source operates at a central wavelength of 930 nm. This system consists of three main parts: a handheld scanning probe, a base unit and a personal computer (PC) (Fig. 1). The base unit contains the SLD light source. A fiber optic coupler is used to direct the light from a broadband SLD source to the Michelson interferometer, which is located inside the handheld probe. The probe and the reference light travel back through the same fiber to the spectrometer and the imaging sensor located in the base unit. The base unit is connected to the PC, which is equipped with two high-performance data acquisition cards. All required data acquisition and processing is performed via the integrated software package, which includes a complete set of functions for controlling data measurement, collection and processing, and for displaying and managing OCT image files. The maximum image depth is 1.6 mm, maximum lateral scanning is 6.0 mm and the axial resolution is 6.2 μm.

2.2. *Marginal integrity evaluation*

Thirty caries-free extracted human pre-molars were selected from the tooth bank after approval from the Human Ethics Committee of the University of Pernambuco, Recife, Brazil. Class I occlusal cavities were prepared with diamond burs (standard grain 75–125 μm, no. 3131, Microdont, São Paulo, Brazil) in a high-speed hand piece with a cooled water spray, using one bur per five cavities. Because of the shape of the bur, slightly expulsive cavities were obtained with the following dimensions: 3 mm mesiodistal width, 1.5 mm buccolingual width and 1 mm occlusal depth. All internal angles were rounded. The teeth were then pumiced and randomly divided into three groups ($n = 10$) according to the resin composite restorative system evaluated (Table 1).

Resin composites were inserted in two oblique increments. Each increment was photoactivated according to the manufacturer's recommendations (Table 1) using a halogen light output (Optilight Plus™/Gnatus, São Paulo, Brazil). Just before each specimen preparation, light intensity was measured with an external radiometer (Gnatus, São Paulo, Brazil), always within the range of 550–600 mW/cm^2.

After storage for 24 h at room temperature in 0.9% saline solution in a dark environment, marginal excesses were removed with an air-cooled, high-speed, fine diamond bur (no. 3118F KG Sorensen, São Paulo, Brazil). Finishing and polishing

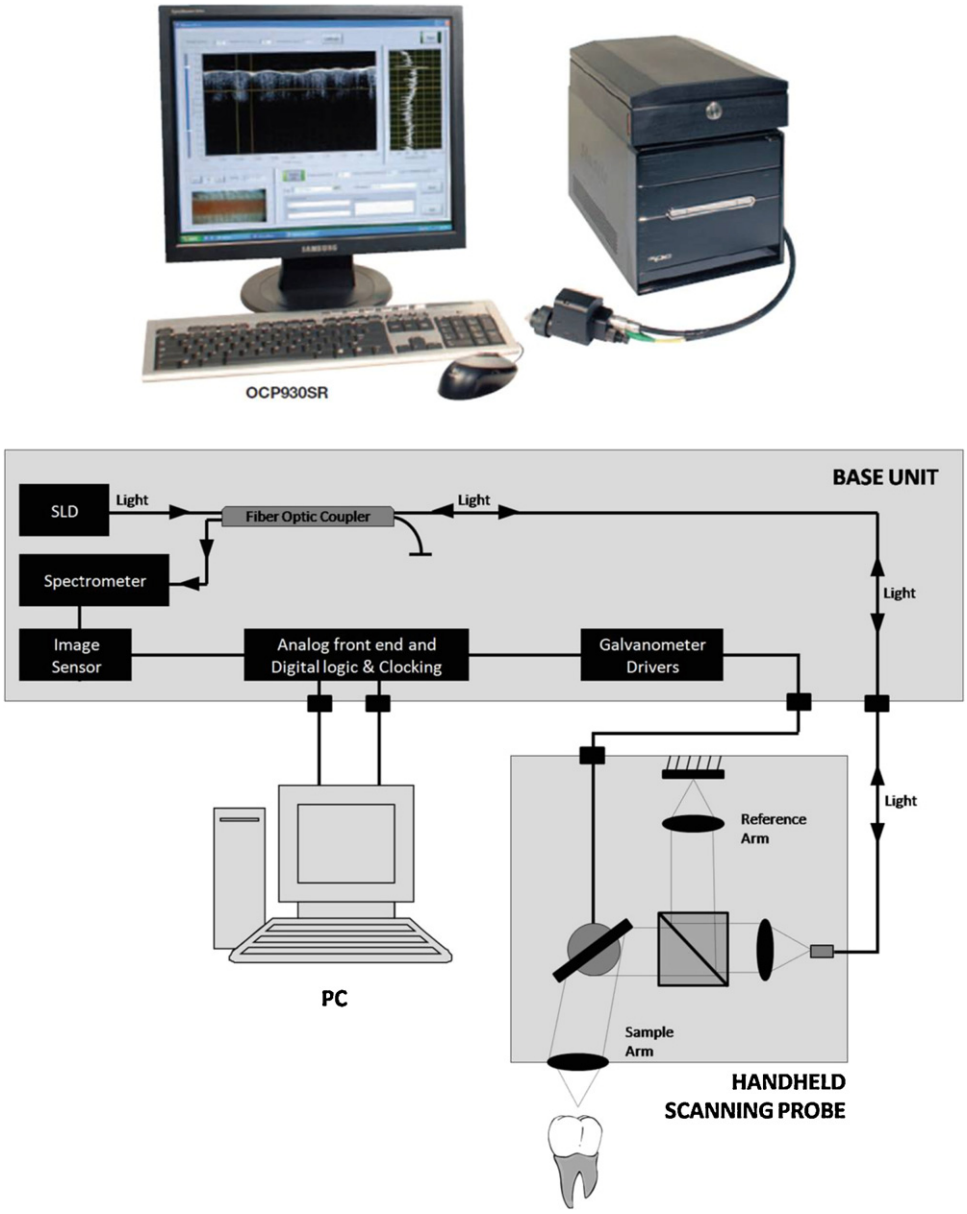

Fig. 1 – Commercial OCT SR-OCT: OCP930SR (Thorlabs, New Jersey, USA).

of the restorations were conducted using low-speed rubber points (Enhance/Dentsply, Rio de Janeiro, Brazil) followed by felt points (Edenta, Hauptstrasse, Switzerland) with extra-fine grain aluminum oxide polishing paste (Diamond R/FGM, Joinville, Brazil). Specimens were then washed with distilled water for 15 min in an ultrasonic bath (Biowash/Bioart Equipamentos Odontológicos, São Carlos, Brazil) to eliminate any debris. After additional 24 h storage in the dark in 0.9% saline solution, the specimens were thermocycled. Alternate baths of $5 \pm 3\,^{\circ}C$ and $55 \pm 3\,^{\circ}C$ were applied at 500 cycles each for 15 s.

Specimens were positioned and individually fixed to the work table with modeling clay. Cross-sectional buccolingual images were obtained every 250 μm from the start of one of the proximal margins to the other. This procedure gave a complete mapping of the internal margins of the restoration.

Images were then qualitatively analyzed using public domain software, Image J (*Imaging Processing and Analysis in Java*) [12]. Whenever doubts on the integrity of internal margins arose, A-scans of specific points were analyzed. Due to the level of noise in OCT images, it was necessary to use a low-pass filter for all images. This kind of filter introduces a distortion in the form of smoothing but is useful to removing isolated lines and pixels while preserving spatial resolution [13]. A 5×5 average filter was used for noise reduction using a special program in the Matlab language. This program also provides A-scans from filtered images of specific points as a function of depth, analyzed using Origin 8.0 (Microcal Software Inc, Northampton, USA). For accurate quantitative measurement throughout OCT, it is necessary to know the refractive index of the materials being studied. Thus, the refractive index of all the test materials was calculated. Samples of the materials

were obtained using a Teflon mold so that the exact thickness of the material could be determined using a digital caliper (0.01 mm). After obtaining the images by OCT, the refractive index could then be determined by applying the formula:

$$\text{Refractive index} = \frac{\text{Optical distance (obtained by OCT)}}{\text{Real distance (mold/caliper)}}.$$

3. Results

Using OCT, it was possible to observe the interactions between the bonding agents and the tooth's substrates. For the conventional two-step bonding agent, Single Bond, a very thin and diffuse zone was observed on dentin after 35% phosphoric acid etching. This corresponds to the structural alterations of the tissues after this procedure. After the Single Bond application (still unpolymerized), initial penetration of the materials into the substrate could be seen. Following polymerization, very few changes were visualized (Fig. 2).

For the two-step self-etching bonding agent, P90 System Adhesive, the interaction of the primer with dental substrates was also observed. The application of a second layer (bond) could also be distinguished by OCT imaging (Fig. 3).

Qualitative analysis of the internal margins did not reveal the presence of gaps although distinctive patterns were found for each restorative system. Filtek Z350 and Z250/Single Bond presented similar OCT images despite the resin composite used. From Fig. 4a,b it is possible to distinguish two layers with different optical densities, identified as the adhesive and the resin composite, very different from the tomograms of the Filtek P90/P90 System Adhesive where a thicker adhesive layer could be observed (Fig. 4c).

Moreover, a very distinct pattern composed of three distinct layers could be seen when analyzing the margins of the cavities in these samples (Fig. 5). Considering that these 2D images are built by a number of interferograms known as A-scans, the evaluation of the interference pattern on the A-scan could help elucidate each layer. A point (line) on the image was selected covering the three layers and the bright clusters and the A-scan was plotted. In an objective way, every time light reaches a different structure other than air, it changes its direction and interference is generated. Graphically, each interference is demonstrated as a peak. Comparing the interference pattern with the images, it was concluded that: point A, corresponded to the air–resin composite interface; point B, the resin composite–bonding agent interface; point C, the bonding agent–dentin interface. The numbers 1, 2 and 3 correspond to resin composite, bonding agent and self-etch primer, respectively.

Reference refractive indexes and those measured for the test materials are listed in Table 2.

Table 2 – The refractive index of the test materials.

Material	Refractive index (η)
Air	1.00
Water	1.33
Single bond	1.4592
Filtek Z250	1.5926
Filtek Z350	1.5623
Self-etch primer (P90 adhesive system)	1.4176
Bond (P90 adhesive system)	1.4863
Dentin	1.5
Filtek P90	1.5924
Enamel	1.6

4. Discussion

OCT is a non-invasive medical diagnostic imaging modality with a high resolution that can give near-histologic images with a safe broadband light source. Recently, OCT has been used in a wide variety of biomedical applications including dentistry. To be useful as a diagnostic technique, OCT images must reliably reproduce the outline of various materials that are placed in or on the tooth. Previous studies have stated that OCT is particularly well suited for imaging the margins of composite restorations, without exposing patients to ionizing radiation [14].

Class I cavities were prepared manually in a standardized manner (3 mm mesiodistally, 1.5 mm buccolingually and 1 mm deep). This depth was determined based on previous results on shrinkage of resin composites evaluated using three methods, one of which was OCT linear analysis [15]. In that analysis, 0.5-mm thick specimens were used. This thickness was determined by previous pilot studies, such that light could penetrate throughout the sample. Thus, considering the restorative resin composites backscattering properties, shallow cavities were created so that all of the restoration and the cavity floor could be imaged. The authors agree that a rapid glance at the figures could cause some misinterpretation, and the reader may have the feeling that the cavities shown were at different depths. Yet, some aspects should be considered in order to clarify the reasons for possible confusion.

First, it must taken into consideration that the images were obtained from one margin to another, so the images taken near the margins (mesial or distal) of the cavities presented shallower depth due to the cross-section obtained by the OCT equipment. Second, the cusps of the premolars were not sectioned. This decision was made in order to simulate clinical conditions, which to a certain extent, also makes image interpretation easier for a professional with little or no experience with OCT images. The maximum image depth (window image) of the system (1.6 mm), the cavity depth and the height of the cusps must also be considered. Several images were taken for each point, modifying the focal distance in order to scan from the tips of the cusps to the bottom of the cavity, thereby allowing reconstruction of the entire tooth. Besides the height of the cusps and the cavity depth, the light scattering inside the substrate also contributes to smaller image penetration depth. However, this procedure produces reflection artifacts on the upper side of the sample. These artifacts are indeed one of the biggest problems on OCT image generation. Because of the height of the premolars cusps, the focal distance was frequently shortened, producing distortion of the cusps tips, as of they were bending (the asterisk in Fig. 5). This also justifies the need to obtain several images in the tooth in the long axis (Y) and then make a composition of these OCT images to reproduce the tooth cross-section.

The refractive index also influences the acquired image. The higher the refractive index, the more difficult it will be for

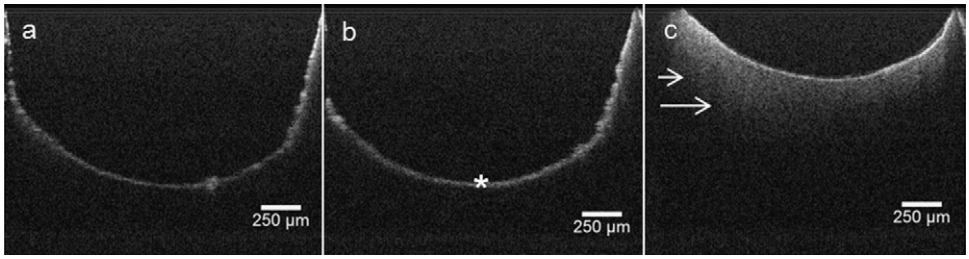

Fig. 2 – Single bond application: (a) prepared cavity and (b) after 35% phosphoric acid etching. Note that the interface line (asterisk) is now thicker than in (a); (c) after single bond application. Note the diffusion of the bonding agent into the dentin substrate (arrows).

light to propagate through an object/sample. This gives the impression that the object/sample is larger than it actually is. Therefore, the closer the refraction index of the object/sample is to that of the air ($\eta = 1.00$), the less image distortion occurs. A classic example of how the refractive index influences the generated image is that of a straw in a glass of water. Part of the straw is in contact with air, which has a refractive index of 1.00, and the lower part of the straw is in contact with water ($\eta = 1.33$). When observing the object, we have the impression that it is thicker in water. In addition, the higher the refractive index, the longer the light will take to propagate through the sample. As image generation is time dependent (acquisition rate is 2.36 frames/s), a sample with higher refractive index will have a greater propagation time, appearing to be thicker.

Finally, different zooming approaches have been used to better present the relevant aspects of each OCT image. For example, in Fig. 3c, a zoom was done beneath the cavity floor to demonstrate the penetration of the bonding agent (P90 adhesive system).

The introduction of new diagnostic imaging requires comparisons with established methods. Such comparisons should take into account factors such as sample preparation, the ease and speed of image acquisition, and the resolution of the system. It is therefore very important that these comparisons are performed using methods with similar resolution. In the case of OCT, it is known that its resolution is closer to that of optical microscopy [11,16,17].

A recently published paper, validated OCT images with confocal microscopy for resin–dentin interfacial gaps [18]. In this study, the authors affirm that the interfacial gaps could be detected in their OCT image; bright clusters formed by bright pixels could be detected at the interface located at the cavity floor. According to the authors, these bright clusters corresponded to higher signal intensity for the SS-OCT (A-scan). Along with the 3D SS-OCT image, an A-scan demonstrated the presence of a gap. As previously mentioned, the OCT image is formed by a series of A-scans, known as a B-scan. Hence each point of the A-scan corresponds to a point in the image and each A-scan peak corresponds to an interface (i.e., contact between different materials, with different refractive indexes). In this way, using the A-scan graph, internal image analysis can be done.

For interfacial gaps, it may be assumed that these gaps are filled with air or in some cases, water. Therefore, for a gap to be considered through A-scan analysis, it is necessary to observe two peaks, one at the resin–air interface and the other at the air–tooth interface. Ideally, measurements of the height and thickness of the gap should be done by A-scan analysis by measuring the distance between these peaks.

The same A-scan interpretation seemed to have been used in this previous study. A-scan analysis indicates two peaks: one for the air–occlusal resin interface and the other for the interfacial gap. Thus, we believe that this second peak actually refers to the tooth–restoration interface without gaps, considering only one peak is shown. In addition, this second peak occurs slightly after 1.5 mm, which is actually the depth of the cavity.

The entire restoration was scanned, that is from one approximal surface to the other including the cavosurface margins. No gaps were observed using this method for all groups, thus accepting both hypotheses. The dark zone underneath the resin composite is occupied by the adhesive layer along with shrinkage (gaps) and handling defects (pores), and it can be concluded that adhesive treatments, apart from regional bonding, improve interfacial wetting of composites

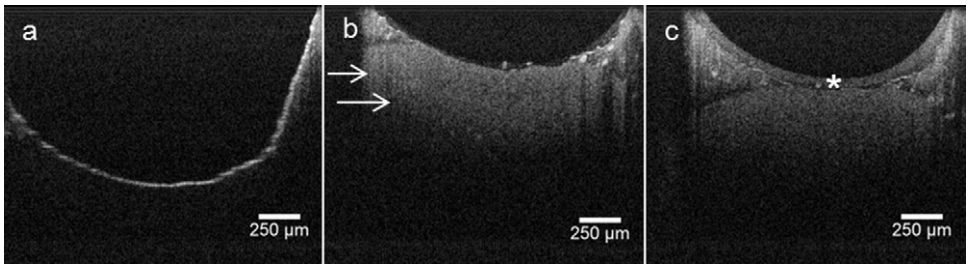

Fig. 3 – The P90 adhesive system: (a) prepared cavity and (b) after self-etching primer application. Note the diffusion of the primer into the dentin substrate (arrows); (c) after bond application. Note the presence of another distinct layer (asterisk).

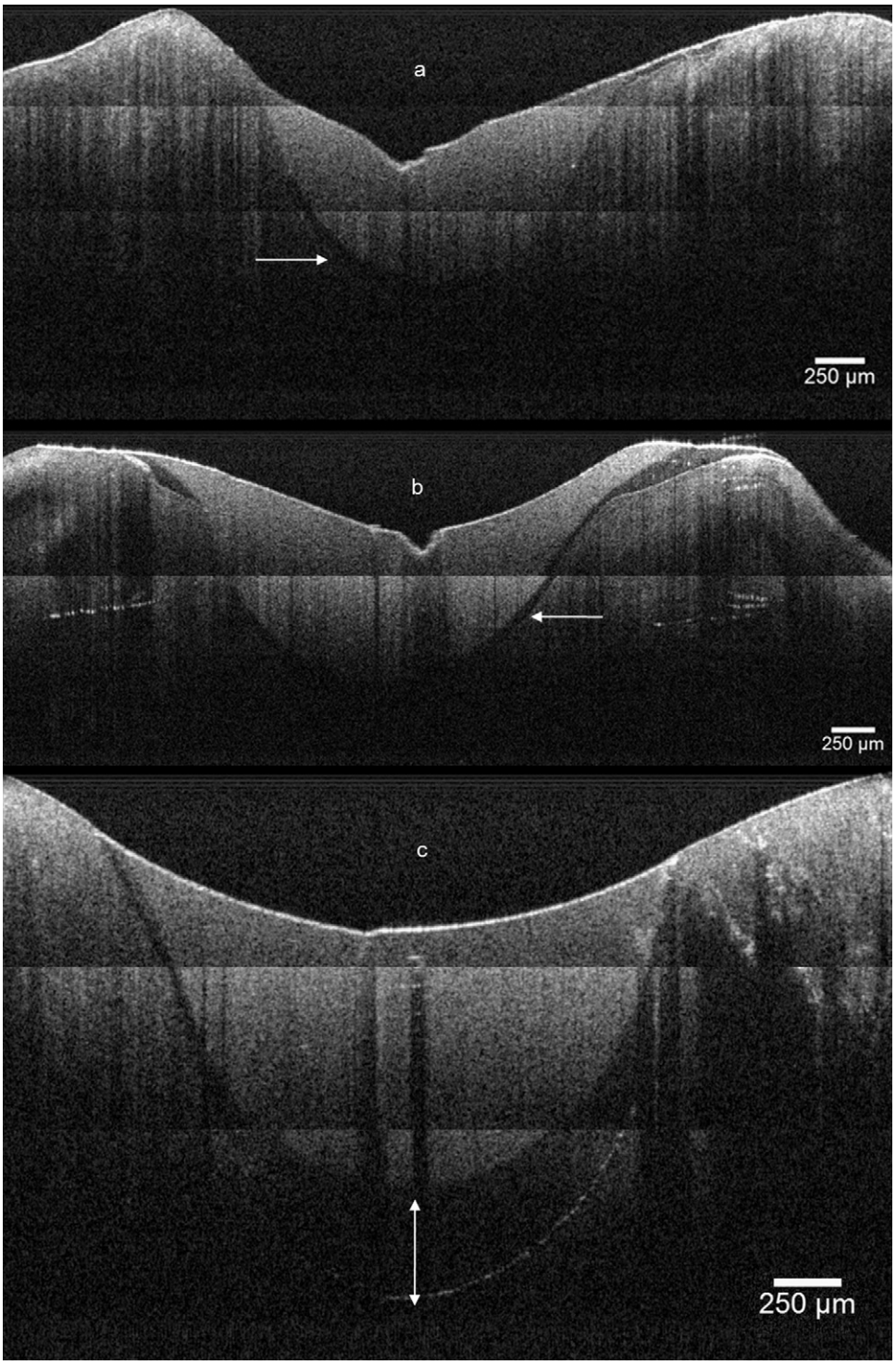

Fig. 4 – (a) Composition of OCT images for a sample restored with Filtek Z250. (b) Composition of OCT images for a sample restored with Filtek Z350. (c) Composition of OCT images for a sample restored with Filtek P90. Note the bonding agent layer (arrows).

to dentin [19]. Nevertheless, images were obtained with the light beam parallel to the long axis of the tooth. So, the light reached the cavity floor perpendicularly, while at the lateral walls images were obtained parallel to light. Further work must be done in order to verify if the direction of the light influences the image obtained.

Interfacial gaps were also identified in restored teeth by an SS-OCT system (wavelength 1260–1360 nm) [20]. However, it is not completely clear whether these darker areas beneath the restorations are gaps filled with air/water or the adhesive layer. Despite the differences in the refractive index of air ($\eta = 1.00$), water ($\eta = 1.33$) and of the bonding agents

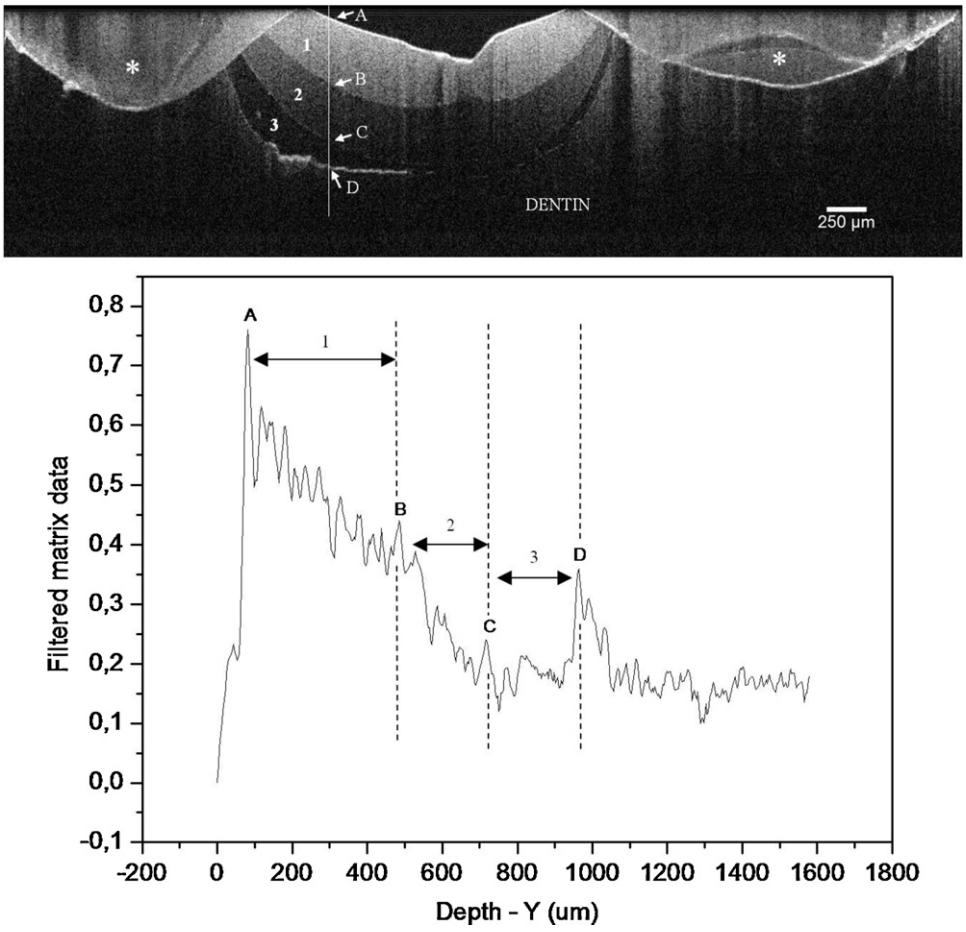

Fig. 5 – OCT image for a sample restored with the Filtek P90 restorative system. For further analysis, A-scan evaluation of the selected point (line) was performed. The numbers refers to layers (1) resin composite, (2) bonding agent, (3) self-adhesive primer. The letters refers to the interfaces: (A) air–resin composite, (B) resin composite–bonding agent, (C) bonding agent–self-adhesive primer, (D) self-adhesive primer–dentin. *Reflection artifacts.

studied here (η = 1.4592–1.4863), it is very difficult to precisely describe what is being observed only by image interpretation. This can lead to misinterpretation and therefore unnecessary restoration replacement. Further analyses of the A-scans are necessary to understand the interfaces present.

Marginal gap formation is the result of localized bond failure and could be attributed to many factors, i.e., cavity configuration, polymerization shrinkage and stress, modulus of elasticity and the adhesive system [21]. Other factors related to the test materials and techniques used must be taken into consideration when comparing experimental set-ups. The performance of one-bottle/all-in-one bonding agent is known to be inferior because its high hydrophilicity adversely affects its long-term stability [22]. It is important to highlight that resin composites were placed in bulk. This induces more stress at the interface, which facilitates gap formation. Also, it was observed that the lowest shrinking materials presented higher volumetric polymerization shrinkage (Filtek P90 = 1.2%; AP-X = 2.21%) [21].

In other studies performed in our laboratory, the presence of these bright clusters was also observed when intentional 50-µm gaps were analyzed by an OCT system [11]. Thus, in our study, special attention was given to the image analysis of these areas. Yet, A-scan analysis could not clearly reveal the presence of gaps in these areas of bright clusters. In Fig. 5, for instance, these bright clusters can be easily observed on the left-hand side of the cavity floor. A-scan analysis was performed at a selected point (line) in order to identify the different layers observed for the Filtek P90 restorative system, but also to verify if there was any interference between the self-adhesive primer and dentin. Some small peaks could indeed be observed, however this observation was not consistent when different A-scans were analyzed for different specimens with bright clusters at the restoration margins. This difficulty could be attributed to noise level of the OCT system even after the use of a low-pass filter. Moreover, images at each step of the application of the bonding systems were also obtained in order to better understand their interaction with the substrate under the OCT.

Validation of OCT images with other methods that require trimming or sectioning must also consider the fact that the cutting surface may deviate from the deepest part of the gap formation that the investigator marked from the SS-OCT test, which might affect the results from different types of gap

investigation [22]. Also, it is very important to highlight that during teeth sectioning, gap formation could occur [23]. Moreover, analysis of sectioned specimens is very limiting, and may not be representative of the whole specimen [21].

Restoration gaps can also be measured in vitro by electron microscopy. Using scanning electron microscopy, several authors have shown that failure gaps in dental restorations can be as narrow as 0.3 μm and can be as wide as 16 μm. The lower limit is beyond the resolution achieved by the OCT system used here (6 μm). Furthermore, the use of OCT has the advantage of showing the restored region as well as the gap, if it exists, and precisely localizing its position [11].

Non-destructive marginal integrity analysis was previously attempted using micro-computed tomography. However, the long data acquisition time can lead to dehydration of the specimens and therefore produce false-positive gap formation or motion artifacts could be present. To date, marginal adaptation is clinically evaluated using conventional or digital radiographs, visual examination and probing with a sharp dental explorer. With ideal radiographic conditions, only translucent areas larger than 40 μm can be detected on radiographs. Moreover, if secondary caries exists around a resin composite restoration, the use of a sharp explorer to detect a slight crevice is neither valid nor reliable and should be avoided [20,23].

Siloranes are a totally new class of compounds for use in dentistry; they are obtained from the reaction of oxirane and siloxane molecules. They have the two key advantages over the individual components: low polymerization shrinkage due to the ring-opening oxirane monomer and increased hydrophobicity due to the presence of siloxane species [15,24].

A dedicated adhesive was produced by the manufacturer to obtain an appropriate bond of silorane composite to dental hard tissues, especially because of the differences in the chemical mechanism of silorane curing compared with methacrylate composites. The P90 Adhesive System is a methacrylate-based, two-step, self-etch system. This bonding system can be considered a mild self-etch adhesive with a pH of 2.7, which produces intense intertubular microporosity with a residual smear layer on the dentin surface and preservation of the smear plugs [5].

In contrast with all other two-step, self-etch systems, the self-etching/primer agent of the silorane adhesive must be polymerized as well as the photopolymerization of the adhesive resin containing a hydrophobic dimethacrylate monomer. The hydrophilic compounds contained within this first step contribute only to the hybrid layer formation, and no mixing occurs between these hydrophilic monomers and the hydrophobic bonding layer. In this way, the coupling between the primed hydrophilic dentin tissue and the extremely hydrophobic silorane-based restorative material can be achieved. Earlier studies have shown that the hydrophobicity of the adhesive layer is also correlated with bond durability. Thus, the hydrophobic coating of the silorane adhesive may provide additional stability to the bonded interface by reducing the amount of water uptake over time [25].

The presence of a thick adhesive layer was observed for the P90 System Adhesive using OCT (Figs. 4 and 5), which is in agreement with previous studies using optical microscopy. This is probably because there is more than one resin application step, which leads to increased thickness of the adhesive layer [19]. SEM evaluations also showed a discernible segregation among the hybrid layer, the adhesive layer, and the bond layer [5,19]. A recently published transmission electron microscopy characterization of a silorane composite bonded to enamel/dentin revealed a typical twofold build up of adhesive resin, resulting in a total adhesive layer thickness of 10–20 μm [26]. However, in our study, this adhesive layer seemed even thicker. Some aspects must be pointed out to explain these differences. The high viscosity of the Filtek P90 dedicated adhesive (self-etch primer and bonding agent) in a small class I cavity favors liquid pooling at the angles in the cavities (especially trihedral), contributing to a much thicker adhesive layer.

The characteristics of the imaging method must also be considered when comparing different imaging methods. For instance, comparisons between images obtained by SEM and OCT must consider the physical principles of each system for image acquisition, resolution and sample preparation. While SEM uses a high-energy beam of electrons (emission of secondary electrons and lower penetration depth), OCT uses light to interact with the sample of interest. This results in differences in image generation and resolution. While SEM reaches nanometer resolution, OCT has micrometer resolution. The differences in the propagation of light and an electron beam must also be taken into account. Moreover, for SEM analysis of dental substrates, special preparation is often necessary, such as sectioning and gold coverage for electrical current discharge. Image generation using SEM is basically based on the interaction of the electrons with the atoms that make up the sample, producing signals that contain information about the sample's surface topography, composition, and other properties such as electrical conductivity. Among the types of signals produced by SEM, secondary electrons are the most common. The gold sputtered layer, necessary for SEM images, can mask details that optical OCT images do not encounter. In addition, alloying or doping can be detected differently by OC compared with SEM, since OCT also deals with the refraction index.

Other characteristics of OCT should be taken into account when trying to interpret these images. Before the analysis, the raw image file has to be resized using image processing analysis programs. In addition, whenever measurements are performed on OCT images, it is necessary to divide the measured value by the refractive index of the materials/sample in order to obtain the real measurements. The reference bar is not given by the system, but can be added by image processing analysis programs. In this case, this bar serves as a lateral reference. For vertical measurements, this reference is not so precise.

The application of the self-etch primer on dentin produced a diffuse image with bright speckles irradiating through into the substrate. This corresponds to intense intertubular decalcification, resulting in an exposed collagen network. A decalcification depth of 1–1.7 μm was previously observed for intertubular dentin associated with a small and incomplete opening of the dentin tubules. This mild pH self-etch primer was unable to completely remove the smear layer, thus the tubules were mostly blocked by smear plugs [5]. Considering the 6-μm resolution of our OCT system, it would be impossible

to detect such small penetration (1–1.7 μm). However, the OCT system detected structural changes at the dentin substrate probably related to loss of mineral content and subsequent changes in the optical properties (refractive index, backscattering properties). In addition, real penetration evaluation using SEM could be masked by the gold metallic shadowing phenomenon. Summarizing, sample preparation for SEM and OCT does not allow us to properly compare sample imaging differences. Optical and electrical penetration depth is not comparable. The much higher thickness observed for the OCT images could provide a new area of research not yet mentioned in the specialized literature.

OCT image interpretation is different compared with radiographs. In radiographic imaging, enamel is more easily observed and therefore is radiopaque; dentin, on the other hand, is more radiolucent. In the case of OCT imaging, this classification based on the tissue radiopacity is unsuitable. Basically this occurs because the tissue interacts with light and the sample does not absorb ionizing radiation. Considering the different mineral densities and consequently different optical properties of the substrates (enamel and dentin) [22], the interaction with light also occurs in a different way. In the case of OCT, the propagation of light depends not only on the tissues refractive index ($\eta_{enamel} = 1.6$, $\eta_{dentin} = 1.5$) but also on its water content. Another important aspect that should be pointed out is that generation of OCT images is mostly based on backscattered light. The polished enamel surface tends to reflect the incident OCT light beam, limiting light propagation into the substrate (dentin). Therefore, for adequate OCT image interpretation, it is crucial for clinicians to receive specific training in order to become familiar with the method.

The main drawback of the technique is the limited penetration depth through dentin substrates and/or dental materials because low backscattering is necessary to generate OCT images. This penetration depth is reliant on the optical properties of the tissue/materials (i.e., refractive index). Furthermore, the greater the depth, the smaller the proportion of light scattering that may be expected. Depth limitations along with signal degradation due to high-scattering nature of dentin results in a dramatic decrease in the sensitivity of detection [22]. Exploitation of the recent advances in OCT in terms of different excitation wavelengths and wider bandwidths can lead to state-of-the-art imaging systems in dentistry, enabling *in vivo*, real-time imaging of both enamel and dentin, which is potentially useful for clinical diagnostics. The development of intra-oral probes that could effectively scan different positions and posterior areas of the oral cavity is also important [23]. The potential of the technique promises fast technological development requiring further laboratory evaluation prior to clinical trials [11].

5. Significance

Considering the characteristics of the OCT system, such as sample preparation, image acquisition and resolution, the setup used in this study was capable of evaluating the marginal integrity of resin composite restorations and detecting some interaction between dental bonding agents and dental substrates. As for the qualitative analysis of internal margins, gaps were not observed regardless of the restorative system. Therefore, OCT can be considered a promising method for the evaluation of the internal margins of restorations *in vivo*.

REFERENCES

[1] 3M ESPE, Filtek LS. Technical profile; December 2008. Available online, from URL: http://solutions.3m.com/wps/portal/3M/en_US/3M-ESPE/dental-professionals/products/category/direct-restorative/filtek-ls.

[2] Mitra SB, Wu D, Holmes BN. An application of nanotechnology in advanced dental materials. JADA 2003;134:1382–90.

[3] Beun S, Gloriex T, Devaux J, Vreven J, Leloup G. Characterization of nanofilled compared to universal and microfilled composites. Dent Mater 2007;23:51–9.

[4] Kleverlaan CJ, Feilzer AJ. Polymerization shrinkage and contraction stress of dental resin composites. Dent Mater 2005;21:1150–7.

[5] Duarte Jr S, Park J-H, Varjão FM, Sadan A. Nanoleakage, ultramorphological characteristics, and microtensile bond strength of a new low-shrinkage composite to dentin after artificial aging. Dent Mater 2009;25:589–600.

[6] Ishikiriama SK, Mondelli RFL. Role of additional retention on marginal adaptation and sealing of large resin composite class II restorations. Oper Dent 2007;32:564–70.

[7] Freitas AZ, Zezell DM, Vieira Jr ND, Ribeiro AC, Gomes ASL. Imaging carious human dental tissue with optical coherence tomography. J Appl Phys 2006;99:024906 [6 pages].

[8] Choo-Smith LP, Dong CCS, Cheghorn B, Hewko M. Shedding new light on early caries detection. J Can Dent Assoc 2009;74:913–8.

[9] Colston Jr BW, Everett MJ, Da Silva LB, Otis LL, Stroeve P, Nathel H. Imaging of hard and soft-tissue structure in the oral cavity by optical coherence tomography. Appl Opt 1998;37:3582–5.

[10] Colston Jr BW, Sathyam US, Da Silva LB, Everett MJ. Dental OCT. Opt Exp 1998;3:230–8.

[11] Melo LSA, Araujo RE, Freitas AZ, Zezell D, Vieira Jr ND, Girkin J, et al. Evaluation of enamel dental restoration interface by optical coherence tomography. J Biomed Opt 2005;10:064027.

[12] Rasband WS. Image J; July 2006. Available online, from URL: http://rsb.info.nih.gov/ij/,1997-2006.

[13] Jain AK. Fundamentals of digital image processing. New Jersey: Prentice Hall; 1989. p. 244–8.

[14] Otis LL, Al-Sadhan RI, Melers J, Redford-Badwal D. Identification of occlusal sealants using optical coherence tomography. J Clin Dent 2003;14:7–10.

[15] Monteiro GQM, Montes MAJR, Rolim TV, Mota CCBO, Kyotoku BBC, Gomes ASL, et al. Alternative methods for determining shrinkage in restorative resin composites. Dent Mater 2011;27:e176–85.

[16] Matheus TCU, Kauffman CMF, Braz AKS, Mota CCBO, Gomes ASL. Fracture process characterization of fiber-reinforced dental composites evaluated by optical coherence tomography, SEM and optical microscopy. Braz Dent J 2010;21:420–7.

[17] Braz AKS, Aguiar CM, Gomes ASL. Evaluation of the integrity of dental sealants by optical coherence tomography. Dent Mater 2011;27:e60–4.

[18] Bakhsh TA, Sadr A, Shimada Y, Tagami J, Sumi Y. Non-invasive quantification of resin-dentin interfacial gaps using optical coherence tomography: validation against

confocal microscopy. Dent Mater 2011, doi:10.1016/j.dental.2011.05.003.
[19] Papadogiannis D, Kakaboura A, Palaguias G, Eliades G. Setting characteristics and cavity adaptation of low-shrinking resin composites. Dent Mater 2009;25:1509–16.
[20] Ishibashi K, Ozawa N, Tagami J, Sumi Y. Swept-source optic al coherence tomography as a new tool to evaluate defects of resin-based composite restorations. J Dent 2011;39:543–8.
[21] Gao B-T, Lin H, Han J-M, Zheng G. Polymerization characteristics, flexural modulus and microleakage evaluation of silorane-based and methacrylate-based composites. Am J Dent 2011;24:97–102.
[22] Senawongse P, Pongprueksa P, Harnirattisai C, Sumi Y, Otsuki M, Shimada Y, et al. Non-destructive assessment of cavity wall adaptation of class V composite restoration using swept-source optical coherence tomography. Dent Mater J 2011;30:517–22.
[23] Makishi P, Shimada Y, Sadr A, Tagami J, Sumi Y. Non-destructive 3D imaging of composite restorations using optical coherence tomography: marginal adaptation of self-etch adhesives. J Dent 2011;39:316–25.
[24] Ilie N, Hickel R. Macro-, micro- and nano-mechanical investigations on silorane and methacrylate-based composites. Dent Mater 2009;25:810–9.
[25] Navarra CO, Cadenaro M, Armstrong SR, Jessop J, Antoniolli F, Sergo V, et al. Degree of conversion of Filtek silorane adhesive system and Clearfil SE Bond within the hybrid and adhesive layer: an in situ Raman analysis. Dent Mater 2009;25:1178–85.
[26] Mine A, De Munck J, Van Ende A, Cardoso MV, Kuboki T, Yoshida Y, et al. TEM characterization of a silorane composite bonded to enamel/dentin. Dent Mater 2010;26:524–32.